Field-Scale Precision: Predicting Grain Yield of Diverse Wheat Breeding Lines Using High-Throughput UAV Multispectral Imaging

Nisar Ali, *Student Member, IEEE*, Ahmed Mohammed, *Student Member, IEEE*, Abdul Bais, *Senior Member, IEEE*, Samia Berraies, Yuefeng Ruan, Richard D. Cuthbert, and Jatinder S. Sangha

***Abstract*—This study explored how to use UAV-based multispectral imaging, a plot detection model, and machine learning (ML) algorithms to predict wheat grain yield at the field scale. Multispectral data were collected over several weeks using the MicaSense RedEdge-P camera. Ground truth data on vegetation indices were collected utilizing portable phenotyping instruments, and agronomic data were collected manually. The YOLOv8 detection model was utilized for field-scale wheat plot detection. Four ML algorithms—decision tree (DT), random forest (RF), gradient boosting (GB), and extreme GB (XGBoost were used to evaluate wheat grain yield prediction using normalized difference vegetation index (NDVI), normalized difference red edge index (NDRE), and green NDVI (G-NDVI) data. The results demonstrated the RF algorithm's predicting ability across all growth stages, with a root-mean-square error (RMSE) of 43 grams per plot (g/p) and a coefficient of determination (R^2) value of 0.90 for NDVI data. For NDRE data, DT outperformed other models, with an RMSE of 43 g/p and an R^2 of 0.88. GB exhibited the highest predictive accuracy for G-NDVI data, with an RMSE of 42 g/p and an R^2 value of 0.89. The study integrated isogenic bread wheat sister lines and checked cultivars differing in grain yield, grain protein, and other agronomic traits to facilitate the identification of high-yield performers. The results show the potential use of UAV-based multispectral imaging combined with a detection model and ML in various precision agriculture applications, including wheat breeding, agronomy research, and broader agricultural practices.**

***Index Terms*—Breeding varieties, field scale, machine learning (ML), plot detection model (YOLOv8), remote sensing, UAV multispectral imaging, wheat, yield prediction.**

I. Introduction

ONE of the United Nations' sustainable development goals is to end hunger by 2030, but current trends indicate that the deliverables of this objective are at risk. As of 2022, around 702–828 million people were undernourished, a 150-million increase since the start of the COVID-19 pandemic [1]. In addition, forecasts indicate that the global population will exceed 10 billion by 2050 [2]. This presents additional challenges for producing more food while preserving resources and reducing crop losses. Wheat, a staple crop that contributes to around 20% of global dietary calories and proteins, is essential in fulfilling global needs for food [3]. Wheat farmers, however, face increasing challenges as a result of significant changes in the climate, demanding the development of wheat varieties that are resistant to a wide range of environmental conditions, including rising temperatures and water dearth [4]. Modern technology could help address some of the challenges that crop production faces [5]. Unmanned aerial vehicle (UAV)-based methods have the potential to provide valuable insights into identifying wheat phenotypes suitable for growing under challenging environmental conditions [6]. The information generated with the use of this technology could aid in the development of wheat varieties that are more resilient and productive, thus helping to address food security challenges worldwide [7].

The crop yield prediction is important to plant breeders and farmers; it is usually possible to determine it at the harvest stage. It is crucial to develop food policies, control food prices, and improve crop management practices such as fertilizer application [8]. This is especially important for small- and medium-sized farms, which make up over 80% of global farmlands. Ensuring food security for the people who heavily depend on these farms is essential due to their widespread distribution worldwide [9]. This is possible by predicting crop yields before harvest to make timely crop management decisions and future marketing plans [10]. For plant breeders, predicting early-stage crop yields in field plots could help to identify improved lines for varietal development and to address potential yield constraints, such as improving genetic gains, generating diversity in genetic material, or improving factors in crop health, including issues with poor soil health, etc. [11], [12]. Early prediction of crop performance for yield to apply intervention measures, including precise fertilization and management, becomes necessary to maintain optimal crop yields and safeguard food security [13], [14].

Manuscript received 24 March 2024; revised 2 May 2024 and 22 May 2024; accepted 28 May 2024. Date of publication 11 June 2024; date of current version 19 June 2024. This work was supported in part by the Saskatchewan Ministry of Agriculture, in part by Saskatchewan Wheat Development Commission, and in part by the Manitoba Crop Alliance through an Agriculture Development Fund Grant 20210626, and in part by the Natural Sciences and Engineering Research Council of Canada Discovery Grant RGPIN-2021-04171. *(Corresponding author: Jatinder S. Sangha.)*

Nisar Ali, Ahmed Mohammed, and Abdul Bais are with the Faculty of Engineering and Applied Science, University of Regina, Regina, SK S4S 0A2, Canada.

Samia Berraies, Yuefeng Ruan, Richard D. Cuthbert, and Jatinder S. Sangha are with Swift Current Research and Development Centre, Agriculture and Agri-Food Canada, Swift Current, SK S9H 3X2, Canada (e-mail: jatinder.sangha2@agr.gc.ca).

Digital Object Identifier 10.1109/JSTARS.2024.3411994

© 2024 The Authors. This work is licensed under a Creative Commons Attribution-NonCommercial-NoDerivatives 4.0 License. For more information, see https://creativecommons.org/licenses/by-nc-nd/4.0/

Remote sensing technology [15], [16] has made significant contributions to various fields, such as resource surveys [17], urban planning [18], national security [19], and agricultural development [20]. Remote sensing has emerged as an efficient method of crop yield prediction because of its advantages in simplicity of data collection, low cost, efficiency, spatial coverage, and short operation cycles [21], [22]. Recent advances in remote sensing technologies have allowed researchers to use UAV-based imaging to study the growth and development of crops, including wheat. By analyzing these images, researchers can extract detailed information about plants' morphological and biological features to determine their performance in different growth environments. This technique provides vital insights into how plants grow and develop, which can improve agricultural practices and crop yields in various growth environments for crop yield reliability [19], [23], [24].

The UAVs commonly have three types of optical sensors: 1) red, green, and blue (RGB); 2) multispectral; and 3) hyperspectral [25]. RGB cameras are inexpensive, but they have a limited number of bands and face challenges in capturing the complete spectrum of the crop canopy [26]. While hyperspectral sensors excel at precisely characterizing spectral responses, they are costly and require complex data processing [27]. Multispectral sensors have recently gained attention in agricultural remote sensing due to their affordability and inclusion of important bands such as red edge and near-infrared (NIR), which are crucial for detecting various agricultural parameters, such as vegetation health, chlorophyll content, crop stress levels, crop biomass, and crop yield estimation [28]. Multispectral imaging operates within the 400–900 nm wavelength range, covering bands, such as RGB, red edge, and NIR [29]. Several vegetation indices (VIs) derived from these bands are often used to evaluate agricultural biophysical parameters. These VIs give detailed information about crop growth and how it reacts to stressors such as diseases, pests, changes in soil moisture conditions and temperature, and in estimating crop yield [30], [31]. Examples of these indices include the normalized difference vegetation index (NDVI) [32], the green NDVI (G-NDVI), the normalized difference red edge index (NDRE), and the enhanced vegetation index (EVI) [33], among others. Many researchers have successfully evaluated crop features and yield using VIs extracted from UAV multispectral images, generating useful information for field application [34], [35].

Accurate crop yield predictions have been demonstrated with UAVs, combining the VIs and growth stages tailored to specific research objectives. For example, Zhou et al. [35] forecasted rice yield using UAV-based RGB and multispectral imagery, highlighting the reliability of airborne VIs for crop growth and yield prediction. Similarly, Zhu et al. [36] employed UAVs with multispectral cameras to capture wheat images at various growth stages, evaluating nine VIs for yield prediction. The crop phenotype analysis identified the heading to grain fill stage transition as optimal and the enhanced vegetation index without a blue band (EVI2) as the most effective feature for yield prediction. Fu et al. [37] used a multispectral camera to capture wheat canopy images at important growth stages and applied machine learning (ML) approaches to estimate yield. These authors discovered a reasonable fit between VIs at jointing, flowering, and grain fill stages and yield, with NDVI at jointing, NDRE at flowering, and canopy chlorophyll content index at grain fill stages as the one providing the best estimates for yield. Shafiee et al. [38] identified NDVI as the highest predictor of wheat yield. Wan et al. [39] developed a rice yield prediction model based on NDVI, normalized difference yellowness index (NDYI), canopy height, and canopy cover utilizing a UAV platform equipped with RGB and multispectral cameras. These investigators determined that the initial heading stage was ideal for yield prediction. All these studies demonstrate that the most effective VIs and growth stages for yield prediction change over the growth season, restricting extrapolation beyond specified time points.

In recent decades, process-based and ML models have been commonly utilized to predict crop yields. Process-based crop models, such as WOrld FOod STudies [40], decision support system for agrotechnology transfer [41], and the agricultural production systems simulator [42], consist of various mathematical functions that explain the physiological processes during crop growth. However, the relationships between crop physiological processes and climate, soil conditions, and management methods accounted for in process-based models demand substantial data inputs, calibration of numerous parameters, and significant time and labor investments, making them more cumbersome [43], [44].

ML algorithms require less initial information about the underlying distribution and model assumptions [45]. Instead, they extract them indirectly from the training dataset, making them useful for various tasks [29], [46], [47], [48]. ML can adapt to different data types, allowing for a better understanding of models and the analysis of complex datasets [49], [50], [51], [52]. These models offer the opportunity to develop crop yield prediction models using multidimensional data [52]. For example, Jeong et al. [53] found that random forest (RF) could predict crop yield more accurately than multiple linear regression (LR). Leng and Hall [54] used RF to predict maize yield variation in the USA and discovered that it outperformed LR. The authors in [55], [56], and [57] demonstrated that ML models could estimate field-scale crop yield utilizing various data sources, guiding in-season management decisions. Moreover, different crop growth phases respond differently to climatic events; for example, the reproductive period in wheat is more sensitive to drought and heat stress due to its direct impact on grain production [56]. Assessing the contributions of climate and remote sensing data at different growth stages is crucial for predicting wheat grain yield [57].

Crop yield assessment in corn, rice, and wheat is generally shown with fixed VIs at a single growth stage, neglecting the input of several crop characteristics at different stages that could add to the grain yield estimation [58]. Optimal combinations of VIs from multiple growth stages can enhance the capability of prediction models [59]. Nevertheless, the stability and applications of yield prediction models at field scales remain understudied, emphasizing the need for accurate predictions to optimize large-scale agricultural management and ensure food security.

In this article, we have utilized UAV multispectral imaging of the experimental field to create RGB images and various VIs. We have gathered a set of VIs weekly throughout the crop growth cycle. This approach allows us to overcome the limitations of relying on fixed VIs at a single growth stage. Weekly VIs help us to have a dynamic understanding of crop characteristics at different stages, which aligns with the concept that the optimal combinations of VIs from multiple growth stages enhance prediction models for crop yield. Additionally, our methodology addresses the challenges of predicting yield at the field scale with wheat plots having different breeding lines with variable yield potential. We aimed to develop accurate prediction models for wheat grain yield by integrating ML techniques with the data gathered from UAV-based multispectral imaging. The main contributions of our work are outlined as follows.

1) *Data collection and imaging:* Gather UAV multispectral imaging data at the field scale, capturing dynamic changes in crop characteristics throughout wheat growth and development.
2) *Utilization of multispectral images:* Utilize UAV multispectral images to generate various VIs weekly, addressing limitations associated with fixed VIs from a single growth stage.
3) *Enhancing prediction models:* Assessing the best ways to combine VIs from different stages of growth to improve models that predict wheat grain yield, focusing on field-scale experiments with breeding lines having diverse agronomic characteristics.
4) *Detection and analysis:* Employ the YOLOv8 detection model to accurately identify wheat plots within the field, enabling precise crop health and vegetative analysis.
5) *ML integration:* Integrate ML algorithms, decision tree (DT), RF, gradient boosting (GB), and extreme GB (XGBoost) with data from UAV-based multispectral imaging to develop accurate prediction models for wheat grain yield.

II. Materials and Methods

This section outlines the experimental setup, data collection procedures, and analytical approaches used in this research to evaluate the dynamics of yield prediction with UAV-based multispectral imaging, a wheat plot detection model, and ML algorithms.

A. Study Area and Field Information

A panel of 30 bread wheat [*Triticum aestivum* L.] lines including near isogenic sister lines (NILs), wheat parents and check cultivars, have been made at Swift Current Research and Development Centre, Swift Current, SK. The NILs were developed from an elite spring wheat breeding population named "B1018" (BW928/BW431/Carberry). The NILs that differ in wheat grain yield and protein concentration were derived from the F_6 family and are homozygous, with an average of over 95% similarity in genetic background. There is, thus, substantially reduced genetic variation in associating genotypes with phenotypes. This bread wheat panel was used as a platform for this phenomics study. These lines were seeded in yield plots that are commonly used by wheat breeders for evaluating advanced lines and selecting genotypes with good agronomics, quality, and disease-resistance packages for advancing as varieties. Field plots were seeded in May 2023 using a randomized complete block design with three replications at Agriculture and Agri-Food Canada's research farm in Indian Head, Saskatchewan. The field plots were seeded under rainfed conditions without any application of irrigation. Each plot measured approximately 10 feet in length and 4 feet in width and was seeded with 1200 seeds in four rows with a gap of 0.75 feet between rows. The gap between plots was filled by seeding two rows of winter wheat. Standard field practices were followed for fertilization, weed, disease, and pest control to minimize other factors in yield limitations. Wheat lines were evaluated for wheat grain yield, protein, and other agronomic characteristics. The wheat grain yield was calculated in grams per plot using a conversion factor. The geographical location of the experimental field is shown in Fig. 1.

B. Data Collection

In this study, we employed the MicaSense RedEdge-P Camera and DJI M300 RTK drone to acquire all image data. The MicaSense RedEdge-P Camera is a specialized six-band multispectral sensor designed for agricultural and environmental monitoring applications. It captures images of a given area across six distinct spectrum bands: 1) blue, 2) green, 3) red, 4) red edge, 5) NIR, and 6) panchromatic. The panchromatic band of the RedEdge-P Camera, boasting a resolution of 2464×2056, covers the entire visible spectrum and offers higher spatial resolution compared to the other bands, which have a resolution of 1456×1088. This feature allows for more detailed and precise imaging of the captured region. For each shot taken by the camera, six files are generated, each containing information captured by one of the six bands. The images are stored in a 16-b TIFF format, ensuring high precision in the recorded data. We collected data over several weeks, gathering approximately 500 aerial images each week from 42 feet above the wheat plots in the field using a UAV.

To ensure the reliability of the UAV-based multispectral data, we implemented specific control measures. Data collection occurred between 11:00 A.M. and 1:00 P.M. on a sunny day. Additionally, we maintained the sensors in a vertical position and conducted calibration of the multispectral sensors before each flight. We employed the agisoft metashape software [60], [61] to generate an orthomosaic of the wheat field and used the geographic information system application [62], [63] for further processing.

1) Yield Ground Truth Data: Ground truth data for agronomic and physiological traits were collected on wheat lines between May 15 and August 22, 2023. The wheat grain yield data were collected after the harvesting for individual plots was completed with a plot harvest combine, and the grain was dried to 13.5% moisture content. Grain yield from all three replicated plots of a wheat line was measured individually using a digital weighing balance (Sartorius, 0.001g sensitivity) and the yield was expressed in grams per plot. We used ground truth data, multispectral images, and postharvest wheat grain

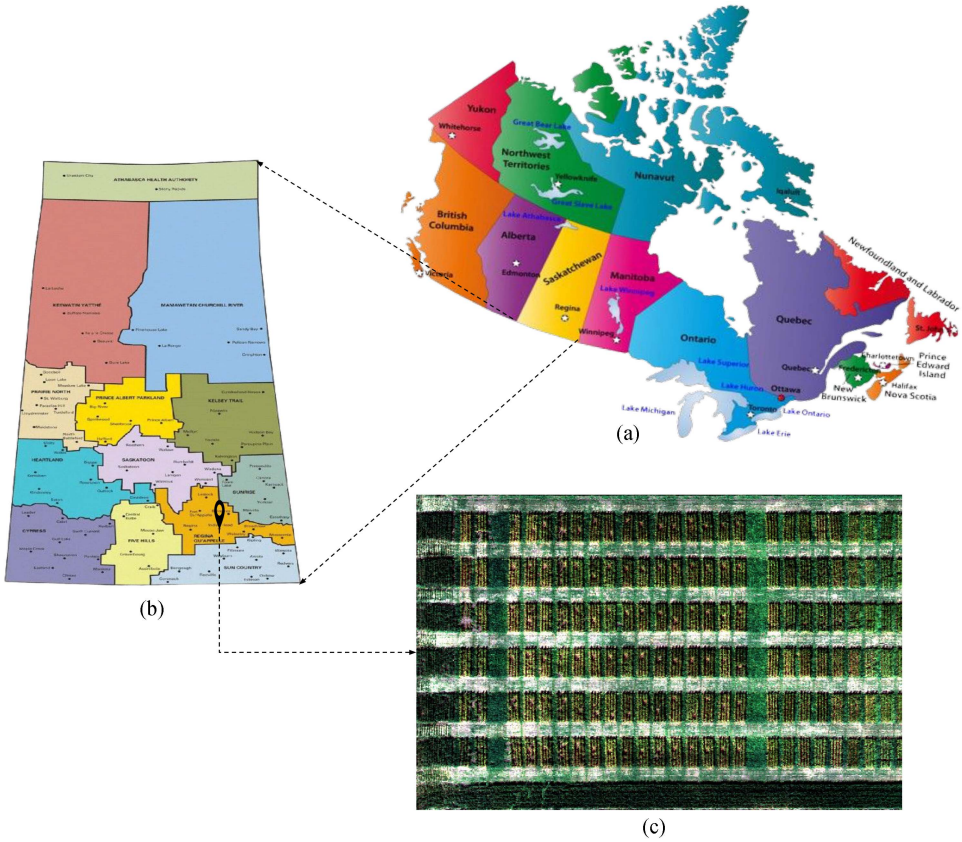

Fig. 1. Illustration of the geographical context and specific locations of the study site in Saskatchewan, Canada, focusing on the Indian Head Agricultural Research Foundation. Panel (a) provides an overview of Saskatchewan within the map of Canada, highlighting its regional placement. In (b), a closer examination zooms in on the Indian Head Research Farm in Saskatchewan, offering a more detailed view of the study area. Finally, panel (c) presents a mosaic of the experimental field, providing a visual representation of the terrain and landscape under investigation and further contextualizing the region where the UAV imaging took place.

yield for the analysis and prediction models reported in this study.

2) VIs Ground Truth Data: Ground truth data for reflectance spectra and VIs were collected weekly from June 24th (booting stage) to August 15th (physiological maturity stage). Using two portable devices, a GreenSeeker fitted with NDVI sensors and the FieldSpec 2 instrument with a spectral range of 350–1100 nm (ASD Malvern Panalytics), we gathered multiple VIs, including NDVI, NDRE, and G-NDVI, from each replicated plot of all the 30 wheat lines at weekly intervals. For both instruments, each plot was scanned between 11:00 A.M. and 1:00 P.M. on a sunny day by keeping the sensors vertically at a fixed distance above the canopy, following the method outlined in [64]. This approach aimed to provide precise ground truth data, which was then compared with calculated UAV multispectral data for yield prediction. The equations for these indices are reported in Table I.

3) UAV-Based RGB and VIs Data: The UAV-based multispectral imaging bands, such as RGB, red edge, and NIR, were essential in our study. The bands were used to create RGB images and VIs data, including NDVI, NDRE, and G-NDVI. The VIs offer valuable information on vegetation characteristics and health, enabling detailed vegetation analysis and helping in predicting yield.

TABLE I
VEGETATION INDICES EQUATIONS

Vegetation index	Equation
NDVI	$\frac{\text{NIR}-\text{Red}}{\text{NIR}+\text{Red}}$
NDRE	$\frac{\text{NIR}-\text{RedEdge}}{\text{NIR}+\text{RedEdge}}$
G-NDVI	$\frac{\text{NIR}-\text{Green}}{\text{NIR}+\text{Green}}$

C. Methodology

Fig. 2 provides the complete framework for the approach used in this study for wheat grain yield prediction. The framework consisted of three stages. To begin with, UAV was utilized for multispectral imaging to collect data, leading to the generation of RGB and VIs images. The RGB images facilitated the detection of field-scale wheat plots while VIs were utilized to create binary masks. The coordinates of detected RGB wheat plots were then overlaid onto the binary masks of VIs. In the second stage, NDVI, NDRE, and G-NDVI were calculated for each detected

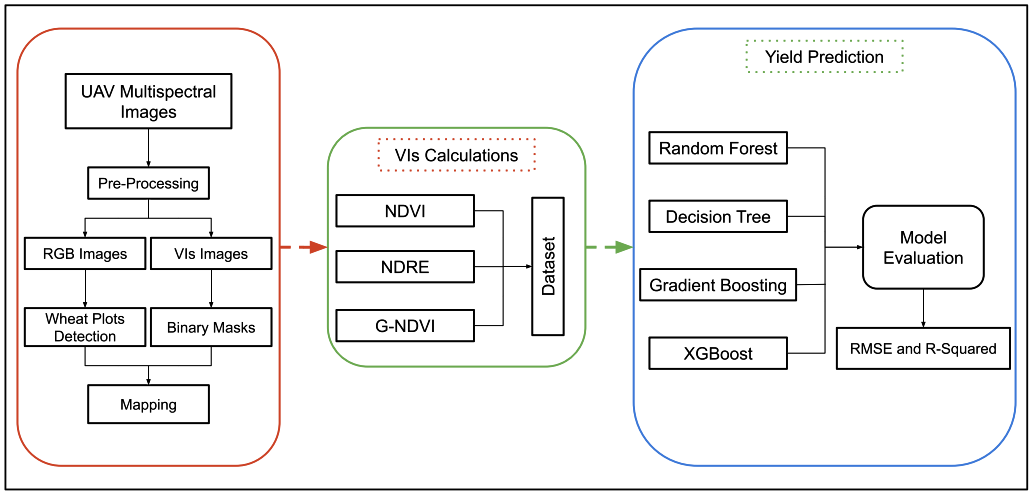

Fig. 2. Conceptual framework of the wheat grain yield prediction model, which includes data from the NDVI, NDRE, and G-NDVI. The model is structured to utilize deep learning specifically for wheat plot detection while employing ML techniques for yield prediction. The model's integration of these diverse data sources and analytical approaches aims to improve the accuracy and robustness of yield predictions, demonstrating an effective approach that leverages the abilities of both deep learning and ML methodologies in agricultural forecasting.

plot. Finally, ML techniques were implemented in the third stage to predict wheat grain yield based on the calculated indices.

1) Wheat Plot Detection: The research methodology involved utilizing UAV multispectral data, which were initially processed to generate RGB images. A band registration and alignment technique was applied to enhance the accuracy of the RGB images. In our research, we adopted a methodology inspired by a study [65] that developed a technique for aligning multispectral bands captured by separate sensors. The process revolved around leveraging image intensity to achieve alignment. Initially, a pair of images, a similarity metric, an optimizer, and a transformation type were specified for the iterative alignment process. The similarity metric evaluated alignment accuracy by generating a scalar value indicative of image similarity while the optimizer fine-tuned alignment by minimizing or maximizing this metric. The transformation type delineated the geometric relationship between the images. Commencing with an internally determined transformation matrix, the moving image was aligned to the fixed image using bilinear interpolation. To find the best calibration parameters through experiments, images were paired with a reference band, such as Band 2 (Green, with a center wavelength of 560 nm and a bandwidth of 27 nm). The study highlighted the efficacy of the "rigid" transformation type in producing optimal alignment results.

The computer vision annotation tool [66] was used to label wheat plots in RGB images for annotations. Following the preprocessing steps, a YOLOv8 deep learning model (YOLOv8n) was employed to detect wheat plots within the RGB images. The dataset comprised 1000 RGB images, divided into a 70:20:10 ratio for training, testing, and validation purposes. The model consisted of 225 layers and 3 011 043 trainable parameters. The computational load of the model is 8.2 GFLOPs. During training, the AdamW optimizer was employed with a learning rate of 0.002 and momentum of 0.9, utilizing distinct parameter groups for weight and bias decay. The model's training, testing, and validation were conducted utilizing Google Colab GPU resources, ensuring computational efficiency and robust performance evaluation. This approach aimed to optimize the detection accuracy of wheat plots in the UAV multispectral imagery. An example of the detected wheat plots is reported in Fig. 3.

2) VIs Binary Masks: Various indices, including NDVI, NDRE, and G-NDVI, were generated weekly using UAV multispectral data. After computing these indices, the next step was to create binary masks for each index. This binary mask generation helped identify spatial patterns and variations in vegetation health over time. The repeated weekly generation of VIs and their associated binary masks was a dynamic tool for monitoring crop growth's temporal dynamics, providing important insights into its growing health. The NDVI image and its corresponding binary mask are shown in Fig. 4.

3) Mapping: The study proceeded to the mapping phase following the successful detection and the creation of binary masks for NDVI, NDRE, and G-NDVI. The RGB-detected coordinates of wheat plots were overlaid on the VIs binary masks. This mapping ensured that the subsequent calculations of NDVI, NDRE, and G-NDVI were limited to the detected wheat plots. This targeted approach was used to derive accurate and focused VI values inside the wheat plots, avoiding the computation of indices for areas surrounding or beyond the wheat plots. The mapping process is demonstrated in Fig. 5.

4) VIs Calculations: After the mapping process, VIs values were calculated for each identified wheat plot using (1). Using this equation for each detected wheat plot in the image resulted in the precise computation of VIs values tailored to each plot, as depicted in Fig. 6. The study used this method to obtain accurate and localized insights into the vegetation health of individual wheat plots, as the calculation was limited to the specified regions, resulting in a more nuanced understanding

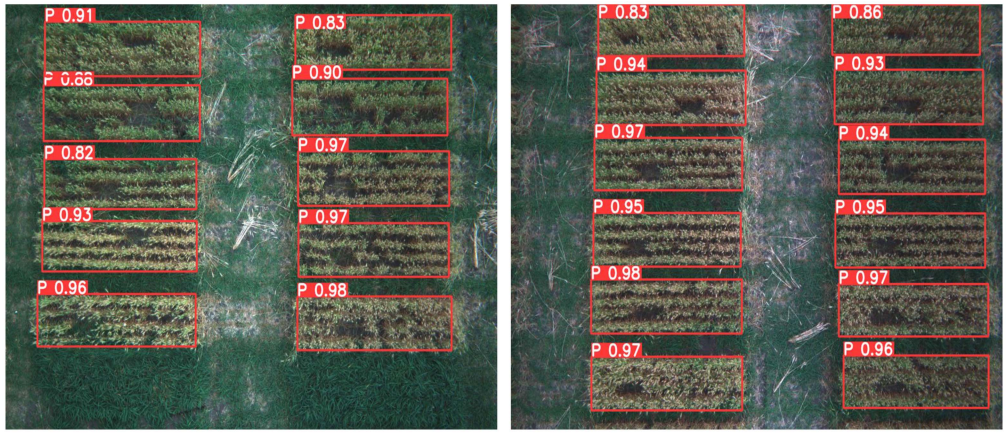

Fig. 3. Detection of wheat plots using the YOLOv8 detection model with UAV-based RGB images. YOLOv8 is used to identify and delineate individual wheat plots in aerial images autonomously. Using UAV RGB-based images provides high-resolution spatial information, allowing for accurate detection of wheat plots.

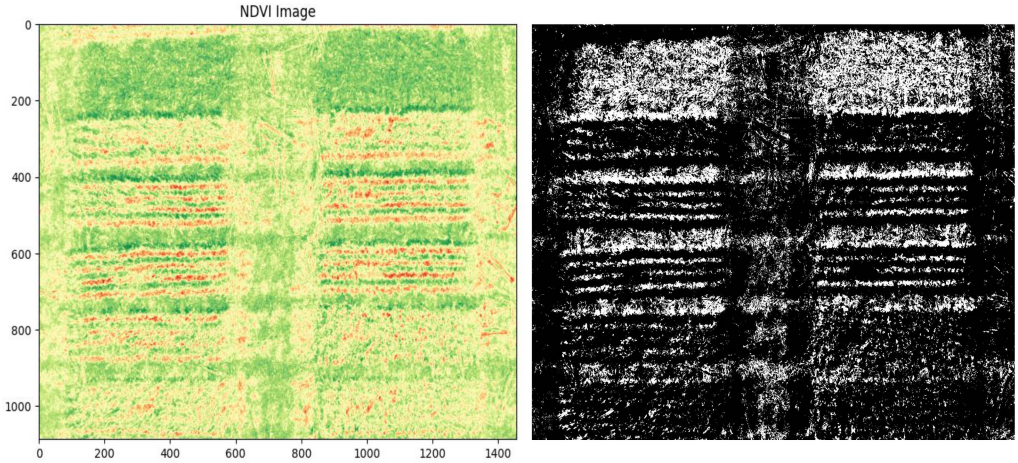

Fig. 4. NDVI image and its corresponding binary mask. The NDVI image, derived from multispectral data, captures the normalized difference in vegetation health, allowing for a visual representation of vegetation density and health across the observed area. The NDVI image is used to generate the accompanying binary mask, which categorizes pixels into binary classes (such as vegetation and nonvegetation). This binary mask is a segmentation tool that helps to delineate and identify specific features or regions of interest in the NDVI image.

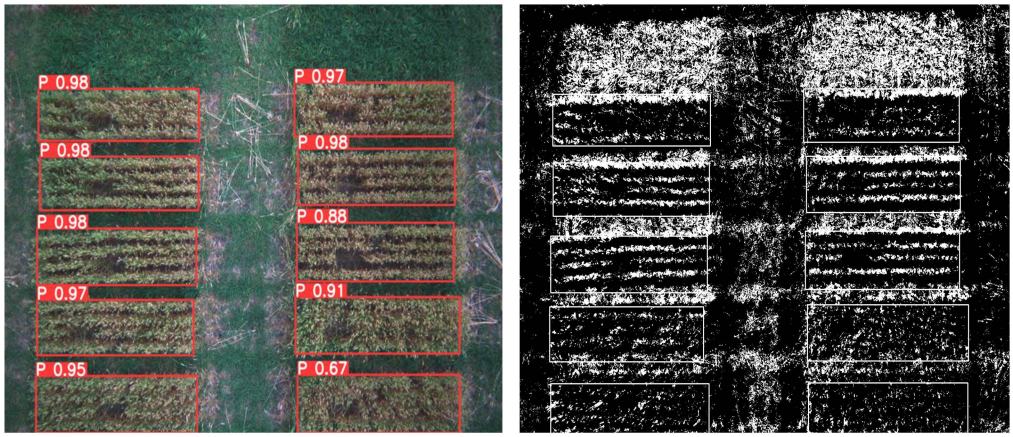

Fig. 5. Mapping the coordinates of wheat plots detected by the YOLOv8 model to the corresponding binary mask derived from the same image. This mapping is undertaken with the specific objective of isolating and delineating the detected wheat plots within the image. The rationale behind this mapping is to facilitate precise computation of VIs strictly within the confines of the identified plots, excluding areas outside them. This targeted approach ensures accurate and focused analysis, allowing for a more nuanced assessment of vegetation health and yield estimation within the detected wheat plots.

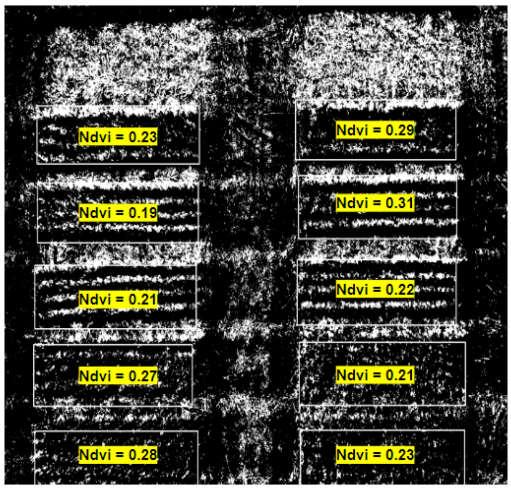

Fig. 6. VIs calculation for each identified plot in the captured image. The goal is to calculate VIs within the detected plots, laying the foundation for subsequent utilization in yield prediction analysis. This method allows a targeted and plot-specific assessment of vegetative parameters, resulting in a more nuanced and accurate crop yield prediction model based on the derived VIs.

of the dynamic agricultural landscape under investigation.

$$\text{veg\_index} = \frac{\sum(V \times M)}{w \times h} \tag{1}$$

where V is the original VI image, M is the binary mask corresponding to the VI image, and $w \times h$ is the width and height of that specific detected wheat plot, respectively.

5) Models Development: We selected four ML-based algorithms, including DT [67], RF [68], GB [69], and XGBoost [70], due to their consistent utilization and demonstrated effectiveness in predicting wheat yield in multiple research studies. The selection of these models was based on their well-documented success in the literature, ensuring a comprehensive approach to yield prediction. DT is a fundamental ML model that recursively splits the data into subsets based on features, aiming to predict the target variable. Each split maximizes the homogeneity of the subsets regarding the target variable, thus forming a treelike structure of decisions [71]. RF, an ensemble method, harnesses the power of multiple DTs. By training several trees on random subsets of the data and features, RF mitigates overfitting and enhances predictive performance [72]. GB is another ensemble technique that sequentially builds a set of weak learners, typically DTs, to minimize the overall error. It iteratively corrects the mistakes of the preceding models, focusing on the instances that were poorly predicted. XGBoost further optimizes GB by employing a scalable and efficient algorithm. XGBoost integrates regularization techniques and parallel computing to boost model performance and speed [73].

The next step involved training the models using three distinct datasets: one for NDVI values, another for NDRE, and the last for G-NDVI. Each dataset was partitioned into training and testing sets, with 70% of the data allocated for training and 30% for testing. This partitioning ensured that the models learned patterns from the training data while allowing for an unbiased evaluation of their performance on unseen data during testing. The models were trained using separate datasets that were designed for each VI. This approach facilitated the evaluation of the predictive capacities of each model concerning distinct VI features. By employing this approach, we acquired a deeper understanding of how each model utilized the unique characteristics of NDVI, NDRE, and G-NDVI datasets to make precise predictions related to wheat grain yield.

6) Models Evaluation: Two metrics were used to evaluate the performance of the models: 1) the root-mean-square error (RMSE) and 2) the coefficient of determination (R^2). The proportion of the dependent variable's variance that can be predicted from the independent variables is measured by R^2. It has a range of 0 to 1, where 1 indicates a perfect fit and 0 means that the model does not explain the target variable's variability in any way beyond the mean. R^2 is determined by using

$$R^2 = 1 - \frac{\sum_{i=1}^{n}(y_i - \hat{y}_i)^2}{\sum_{i=1}^{n}(y_i - \bar{y})^2} \tag{2}$$

where y_i represents the actual wheat grain yield values, $\hat{y}_i$ represents the predicted wheat grain yield values, $\bar{y}$ represents the mean of the actual yield values, and n represents the number of observations in the dataset.

RMSE, on the other hand, is a measure of the average deviation between predicted and actual values. It provides a meaningful interpretation of the model's predicted accuracy using the same units as the target variable. The RMSE is calculated as the square root of the average of the squared differences between predicted and actual values and is reported in

$$\text{RMSE} = \sqrt{\frac{1}{n}\sum_{i=1}^{n}(y_i - \hat{y}_i)^2}. \tag{3}$$

III. Results

In this section, we presented the outcomes of our study into the predictive capabilities of ML algorithms concerning wheat grain yield using three distinct VIs: 1) NDVI, 2) NDRE, and 3) G-NDVI. Our analysis employed four prominent ML algorithms: 1) DT, 2) RF, 3) GB, and 4) XGBoost. The dataset of each index was further categorized into three subsets, each capturing different stages of wheat growth: all-week data, heading to the mid-dough stage data, and mid-dough to the hard-dough stage data.

Dividing the dataset into three different stages in our study offered several potential benefits. It provided stage-specific insights into the predictive capabilities of ML algorithms and the effectiveness of various VIs at different points in the crop growth cycle. It enabled a more granular evaluation of model performance across different growth stages, allowing us to assess how well the algorithms performed at each stage and identify any variations or challenges encountered as the crop matured. This approach helped in optimizing model selection by determining which algorithms and VIs were most effective at different stages, guiding the selection of the most suitable models for accurate yield prediction.

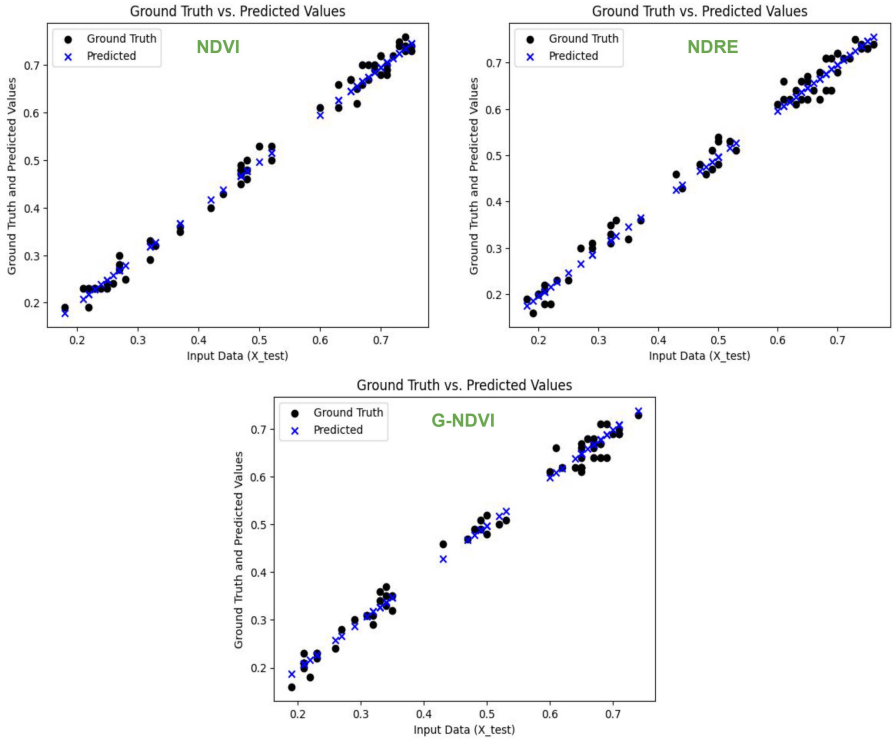

Fig. 7. Use of LR with three VIs: 1) NDVI, 2) NDRE, and 3) G-NDVI. This analysis compares UAV-based calculated VIs to ground-truth VIs data obtained from handheld devices. Each subplot in the figure represents one VI and presents the results of an LR model applied to model the relationship between the calculated VIs and the corresponding ground truth data. These LR models aim to capture and quantify the relationship between the calculated and ground truth VIs, providing insight into the degree of correlation.

A. LR Analysis

We used LR analysis to evaluate the correlation between VIs obtained from UAV and ground truth data acquired from handheld devices in the field. Our study focused on three different VIs: 1) NDVI, 2) NDRE, and 3) G-NDVI. The performance of the LR model was evaluated by using the R^2 metric and the mean-squared error (MSE). We aimed to investigate whether the calculated UAV-based VIs could reliably predict wheat grain yield. The results of LR established strong correlations between the calculated VIs and the ground truth data. About NDVI, the model showed an R^2 value of 0.988% and a low MSE of 0.00039. In the same way, the NDRE dataset exhibited an MSE of 0.00044 and an R^2 value of 0.986%. In addition, the G-NDVI model exhibited a significant R^2 value of 0.983% and an MSE of 0.0005. The findings underscore the strength of the LR approach in capturing the correlation between UAV-based calculated VIs and ground truth data. This analysis highlights the potential utility of indices obtained from UAV in predicting wheat grain yield with precision, as depicted in Fig. 7.

B. NDVI Data Performance

Based on the analysis of the NDVI datasets across different growth stages, it was evident from the results reported in II that RF outperformed other models at each stage of crop growth. For all-week data, RF achieved an RMSE of 43 grams per plot (g/p) and an R^2 value of 0.90, indicating its predictive accuracy compared to other models. During the heading to the mid-dough stage, RF had the lowest RMSE of 39 g/p and the highest R^2 value of 0.89, indicating its efficacy in capturing crop dynamics at this important growth stage. However, at the mid-dough to the hard-dough stage, RF maintained competitive performance but had a larger RMSE of 61 g/p and an R^2 value of 0.73 than in previous stages. Nonetheless, RF emerged as the preferred model for analyzing NDVI data, particularly during the early to medium stage of crop growth, when its ability to predict was most pronounced. The results of the testing stage for each model are presented in Table II.

C. NDRE Data Performance

The NDRE dataset was divided into subsets, and each ML model performed differently at different crop growth stages. While RF and DT competed across all subsets, GB and XGBoost produced more variable results. For the all-week data subset, XGBoost was the most effective model, with an RMSE of 42 g/p and an R^2 value of 0.87, indicating higher prediction accuracy. Conversely, at the heading to the mid-dough stage, DT had the lowest RMSE of 43 g/p and the highest R^2 value of 0.88, demonstrating its usefulness in capturing crop dynamics. In the mid-dough to the hard-dough stage, RF maintained performance with an RMSE of 54 g/p and an R^2 of 0.81 while DT performed well with an RMSE of 52 g/p and an R^2 of 0.84. GB and XGBoost, on the other hand, showed comparable predictive accuracy during this stage, with larger RMSE values and lower R^2 values than RF and DT, respectively.

TABLE II
WHEAT GRAIN YIELD PREDICTION PERFORMANCE ON NDVI DATA

Model	**Performance on different data stages**		
	All-week	Heading to mid-dough	Mid-dough to hard-dough
	RMSE (g/p) / R^2		
RF	43 / 0.90	39 / 0.89	61 / 0.73
DT	47 / 0.88	48 / 0.86	58 / 0.77
GB	46 / 0.88	48 / 0.89	60 / 0.75
XGBoost	49 / 0.85	51 / 0.87	55 / 0.77

TABLE III
PERFORMANCE OF WHEAT GRAIN YIELD PREDICTION ON NDRE DATA

Model	**Performance on different data stages**		
	All-week	Heading to mid-dough	Mid-dough to hard-dough
	RMSE (g/p) / R^2		
RF	50 / 0.86	51 / 0.85	54 / 0.81
DT	49 / 0.88	43 / 0.88	52 / 0.84
GB	46 / 0.87	48 / 0.85	65 / 0.79
XGBoost	42 / 0.87	55 / 0.83	67 / 0.75

TABLE IV
G-NDVI DATA WHEAT GRAIN YIELD PREDICTION PERFORMANCE

Model	**Performance on different data stages**		
	All-week	Heading to mid-dough	Mid-dough to hard-dough
	RMSE (g/p) / R^2		
RF	53 / 0.86	45 / 0.86	42 / 0.86
DT	51 / 0.84	43 / 0.84	56 / 0.81
GB	42 / 0.89	56 / 0.86	65 / 0.80
XGBoost	47 / 0.87	48 / 0.88	50 / 0.82

The findings for the NDRE data of each model are reported in Table III.

D. G-NDVI Data Performance

Analyzing the G-NDVI dataset revealed significant performance trends among the evaluated ML models at various crop growth stages. GB outperformed other models on the all-week data subset, with an RMSE of 42 g/p and an R^2 value of 0.89, showing good prediction accuracy. During the heading to the mid-dough stage, DT had the lowest RMSE of 43 g/p and a decent R^2 of 0.84, demonstrating its ability to capture the heading to the mid-dough stage crop changes. RF performed well from the medium to harvesting stage, with the lowest RMSE of 42 g/p and an R^2 of 0.86, indicating its reliability in predicting crop yield throughout this important growth stage. However, DT performance dropped at this stage, with a higher RMSE of 56 g/p and a lower R^2 of 0.81. While XGBoost performed consistently across all subsets, its predictive accuracy was marginally lower than that of GB and DT. Notably, XGBoost performed well in the heading to the mid-dough stage, with an RMSE of 48 g/p and an R^2 of 0.88. The results are discussed in detail for every model in Table IV.

E. Observations

Here, we presented our observations on the performance of these models at various stages of wheat growth.

Upon evaluation of the NDVI dataset, it was clear that all models performed well at two important stages: 1) all-week data

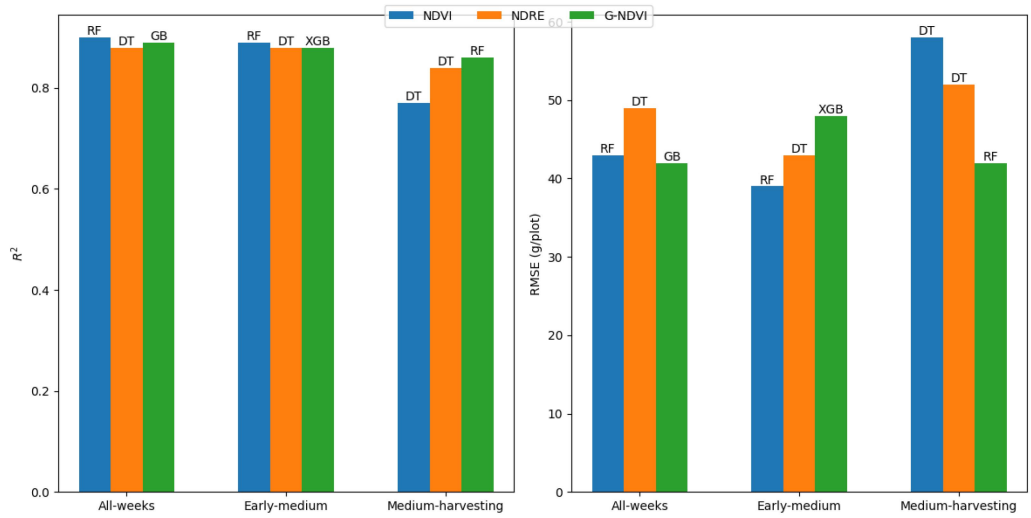

Fig. 8. Performance trends of the best models using the R^2 and RMSE metrics on subsets of NDVI, NDRE, and G-NDVI data. The line graphs depict the models' comparative efficacy in capturing and predicting variations within the NDVI, NDRE, and G-NDVI data.

and 2) the heading to the mid-dough stage data. The models predicted wheat grain yield throughout these stages, as evidenced by their low RMSE and high R^2 coefficient values. However, there was a decrease in performance throughout the mid-dough to the hard-dough stage data, demonstrating a relative deficiency in predicting wheat production in the later stages of growth when the grain is maturing and the chlorophyll reduces due to ongoing senescence activities.

Contrary to the observed decline in performance during the mid-dough to the hard-dough stage data in the NDVI dataset, the models performed consistently across all stages in the NDRE dataset. Notably, the models outperformed the NDVI dataset regarding prediction during the later wheat growth stages. This result demonstrated that NDRE data might be used to predict wheat grain yields precisely, particularly during advanced growth phases when the vegetation contrast is more detectable with multispectral data.

The G-NDVI dataset revealed promising results across all stages of wheat, with the models demonstrating high predictive accuracy. The models' performance in the later stages was notable, highlighting the potential utility of G-NDVI data for predicting wheat grain yield throughout later growth stages. These findings suggested that while NDVI may be useful for early-stage predictions, G-NDVI emerged as a good choice for predicting yield later in the growth phase.

Our findings highlighted the varied performance of prediction models across diverse datasets and growth stages. Although each dataset had several advantages, choosing the right dataset depended on the precise requirements of the prediction task and the stage of wheat growth under consideration. Graphical representations were used to highlight and clarify the identified trends. Fig. 8 shows the models' performance trends across different datasets and growth stages.

Based on the results obtained for wheat grain yield prediction using different models across various stages, RF consistently performed well across all stages for NDVI, NDRE, and G-NDVI data. For NDVI data, RF yielded the lowest RMSE of 43 g/p with an R^2 value of 0.90 across all-week data, whereas, for NDRE and G-NDVI, it achieved the lowest RMSE of 50 g/p and 53 g/p, respectively, for all-week data. Interestingly, at the heading to the mid-dough stage, RF maintained competitive performance across all datasets. However, the GB model generally exhibited higher RMSE values at the mid-dough to the hard-dough stage, indicating reduced predictive accuracy compared to other stages. In the case of the G-NDVI, the mid-dough to the hard-dough subset, RF also showed promising results. Overall, RF emerged as a robust model for wheat grain yield prediction.

IV. Discussion

Our research illustrated the effective utilization of UAV-based multispectral imaging, a wheat plot detection model, and ML algorithms to predict wheat grain yield at a field scale. Our findings indicated that using ML models in combination with various VIs datasets could accurately predict wheat grain yield within specific field plots (field scale). Wheat breeders commonly use these wheat yield plots during the evaluation of a large number of lines to assess grain yield and other agronomic traits [74]. The development of a high-throughput yield prediction model at the field plot scale is highly useful in varietal development programs.

The use of UAV-based multispectral imaging, a plot detection model, and ML algorithms was useful in predicting wheat grain yield at the field scale. Earlier studies mostly focused on estimating wheat yields at larger geographic scales, such as the county level. Han et al. [75] used RF, SVM, and Gaussian process regression (GPR) approaches to achieve R^2 values greater than 0.75 for county-level yield predictions. Similarly, Wang et al. [76] used convolution neural networks (CNN) and long short-term memory (LSTM) to predict winter wheat yields, with good performance metrics (R^2: 0.74, RMSE: 721 kg/ha). Cao et al. [77] used RF and three deep learning models (CNN,

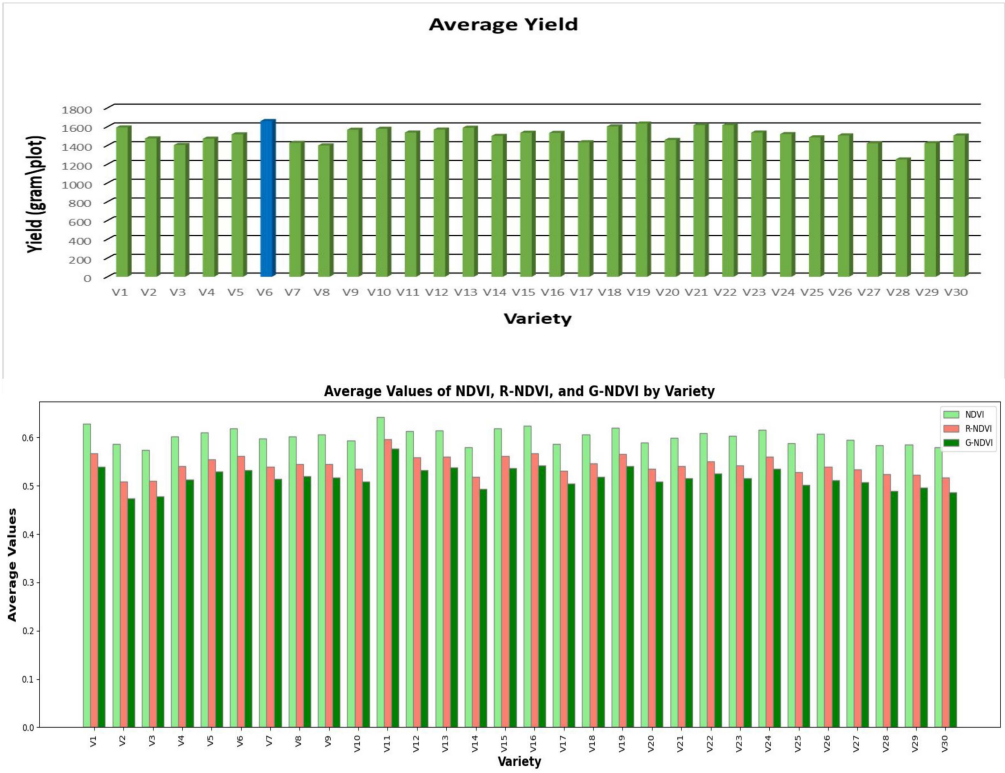

Fig. 9. Figure presents two plots: One displaying the average yield across all varieties while the other illustrates average values of VIs, including NDVI, NDRE, and G-NDVI.

LSTM, and deep neural networks) to estimate wheat yields across 629 counties from 2011 to 2015. They achieved R^2 values greater than 0.85 and RMSE less than 768 kg/ha. From 2011 to 2013, their field-scale projections ranged from R^2: 0.48 to 0.71 and RMSE: 956 to 1620 kg/ha at 87 sites. Notably, predicting yields at the field scale was more difficult due to varied environmental conditions, even within the same county, demanding better resolution datasets [78]. Our RF model, conducted at a field scale, yielded comparable predictive outcomes to previous county-level studies. These yield plots are highly important for the wheat breeders to determine the agronomic performance in multienvironment trials before selecting lines for cultivar release. The automated detection of yield with our method could help to assess accurate yield in hundreds of lines in a short time.

Among the ML models evaluated for wheat grain yield prediction, RF emerged as the top performer across different growth stages, maintaining high predictive accuracy [79], [80], [81]. The RF model based on NDVI data demonstrated good performance, with an RMSE of 43 g/p and an R^2 value of 0.90, indicating its effectiveness in capturing wheat grain yield dynamics throughout the growth cycle. In contrast, the DT model outperformed others when utilizing NDRE data, achieving an RMSE of 43 g/p and an R^2 of 0.88, indicating its fit for specific growth stages. G-NDVI data, when analyzed with GB, exhibited the highest predictive accuracy, yielding an RMSE of 42 g/p and an R^2 value of 0.89. These findings highlight the importance of using appropriate models, and VIs adapted to different growth stages for accurate yield prediction, with RF generally performing well across various conditions.

We observed that wheat grain yield prediction models performed differently across stages and VIs datasets [82], [83]. For the NDVI dataset, models performed well throughout the all-week and the heading to the mid-dough stages, predicting wheat grain yield with low RMSE and high R^2 values [84]. However, their performance dropped from the mid-dough to the hard-dough stage, indicating difficulties in predicting yield during later growth stages. Models utilizing the NDRE dataset, on the other hand, outperformed the NDVI dataset during later growth stages. This indicated that NDRE data may be more accurate for predicting wheat grain yield in mature growth stages. Moreover, the G-NDVI dataset provided positive results across all stages, showing its potential use in predicting yield in later growth stages. These findings underscore the importance of considering the stage-specific performance of VIs in wheat grain yield prediction, with NDRE and G-NDVI emerging as valuable choices for later growth stages.

The importance of VIs in this study cannot be overstated. The VIs change with crop growth stages, and it is more prominent from the anthesis to the physiological maturity stage [85]. We found wheat growth dynamics by using three different indices: NDVI, NDRE, and G-NDVI. Each index provided different perspectives on crop health and development, allowing for precise predictions of yield outcomes. Our findings highlighted the importance of combining multiple indices for an in-depth knowledge of crop dynamics in the context of precision agriculture. We captured complex changes in wheat growth patterns across different stages of development by combining many VIs.

This underlines the need to consider stage-specific performance metrics when selecting appropriate yield prediction indices.

For this study, 30 bread wheat plants that were genetically similar were used. These plants were called isogenic sister lines and came from a spring wheat breeding population called "B1018" (BW928/BW431/Carberry). These sibling lines demonstrate disparities in both grain yield and protein concentration. Breeders specifically used these uniform, replicated yield plots to assess the performance of advanced wheat lines in comparison to check varieties. The overarching objective was to identify and choose lines that displayed desirable agronomic features for improved grain yield, high grain protein for en-use quality attributes, and canopy-reflectance-based differences in indices for estimating nitrogen use efficiency. Significantly, out of these 30 lines, Line # 6 exhibited high-yield performance in all replicated plots. To enhance understanding of our analysis, we included visual depictions of the mean yield and the mean values for NDVI, NDRE, and G-NDVI for different weeks in Fig. 9.

The ML algorithms evaluated in the study, including RF, DT, GB, and XGBoost, demonstrated strong predictive capabilities across different growth stages and vegetation indices. These algorithms showed high accuracy in predicting wheat grain yield, with RF consistently performing well. The use of various vegetation indices such as NDVI, NDRE, and G-NDVI provided valuable insights into crop health and development, enhancing the accuracy of yield predictions. However, potential limitations include the need for further validation across diverse environmental conditions and crop varieties to ensure generalizability. Additionally, the study's reliance on UAV-based multispectral imaging may pose challenges related to data acquisition and processing, requiring careful calibration and validation procedures. Future work should focus on integrating higher-resolution datasets, expanding the geographic scope of the study, and exploring the use of additional ML models to further enhance prediction accuracy.

V. Conclusion

Our study investigated the integration of UAV-based multispectral imaging, a plot detection model, and ML methods for predicting wheat grain yield at the field scale. This approach offers valuable insights into precision agriculture applications, especially in wheat breeding and agronomy research. Utilizing the MicaSense RedEdge-P Camera and various models, including YOLOv8, RF, DT, GB, and XGBoost, we obtained significant insights into crop health and development, enhancing the accuracy of yield predictions. Notably, the RF algorithm demonstrated excellent performance, particularly during the heading to the mid-dough growth stages.

The effectiveness of our approach was further validated by LR analysis, highlighting strong correlations between calculated VIs and ground truth data. Our findings underscored the variability in model performance across datasets and growth stages, emphasizing the importance of selecting appropriate models and VI datasets tailored to specific wheat growth stages. We were also able to compare wheat varieties with different agronomic traits, such as differences in grain yield, by combining isogenic sister lines from a spring wheat breeding population. This approach facilitated the identification of high-yield performers, showcasing the potential of our methodology in selecting promising wheat cultivars for cultivation.

Our study emphasizes the significance of precision agriculture methods in improving crop management strategies and increasing agricultural productivity. By integrating UAV-based multispectral imagery, a wheat plot detection model, ML algorithms, and comprehensive datasets, we offer valuable insights into optimizing wheat grain yield production and informing agricultural decision-making. Our research has implications for agricultural stakeholders, providing farmers and breeders with the necessary resources to make informed choices and adapt to changing environmental conditions.

Acknowledgment

Their invaluable assistance and resources greatly contributed to the completion of this project. Additionally, we extend our gratitude to Agriculture and Agri-Food Canada's cereal staff for their support in field management and phenotyping.

References

[1] "Eradicate hunger." *FN-SAMBANDET*, Feb. 2023. [Online]. Available: https://fn.no/om-fn/fns-baerekraftsmaal/utrydde-sult

[2] E. P. Rosa and J. Ramos-Martín, *Elgar Encyclopedia of Ecological Economics*. Northampton, MA, USA: Edward Elgar Publishing, 2023, doi: 10.4337/9781802200416.

[3] M. J. Iqbal, N. Shams, and K. Fatima, "Nutritional quality of wheat," in *Wheat*, M. ur Rahman Ansari, ed. Rijeka, Croatia: IntechOpen, 2022, ch. 15, doi: 10.5772/intechopen.104659.

[4] L. Murken and C. Gornott, "The importance of different land tenure systems for farmers' response to climate change: A systematic review," *Climate Risk Manage.*, vol. 35, 2022, Art. no. 100419, doi: 10.1016/j.crm.2022.100419.

[5] M. Javaid, A. Haleem, I. H. Khan, and R. Suman, "Understanding the potential applications of artificial intelligence in agriculture sector," *Adv. Agrochem*, vol. 2, no. 1, pp. 15–30, 2023, doi: 10.1016/j.aac.2022.10.001.

[6] L. Feng, S. Chen, C. Zhang, Y. Zhang, and Y. He, "A comprehensive review on recent applications of unmanned aerial vehicle remote sensing with various sensors for high-throughput plant phenotyping," *Comput. Electron. Agriculture*, vol. 182, 2021, Art. no. 106033, doi: 10.1016/j.compag.2021.106033.

[7] P. C. Pandey and M. Pandey, "Highlighting the role of agriculture and geospatial technology in food security and sustainable development goals," *Sustain. Develop.*, vol. 31, no. 5, pp. 3175–3195, 2023. [Online]. Available: https://onlinelibrary.wiley.com/doi/abs/10.1002/sd.2600

[8] C. Bian et al., "Prediction of field-scale wheat yield using machine learning method and multi-spectral UAV data," *Remote Sens.*, vol. 14, no. 6, 2022, Art. no. 1474, doi: 10.3390/rs14061474.

[9] L. H. Samberg, J. S. Gerber, N. Ramankutty, M. Herrero, and P. C. West, "Subnational distribution of average farm size and smallholder contributions to global food production," *Environ. Res. Lett.*, vol. 11, no. 12, Nov. 2016, Art. no. 124010, doi: 10.1088/1748-9326/11/12/124010.

[10] J. Liu et al., "Crop yield estimation in the Canadian prairies using terra/MODIS-derived crop metrics," *IEEE J. Sel. Topics Appl. Earth Observ. Remote Sens.*, vol. 13, pp. 2685–2697, 2020, doi: 10.1109/JSTARS.2020.2984158.

[11] S. M. M. Nejad, D. Abbasi-Moghadam, A. Sharifi, N. Farmonov, K. Amankulova, and M. László, "Multispectral crop yield prediction using 3D-convolutional neural networks and attention convolutional LSTM approaches," *IEEE J. Sel. Topics Appl. Earth Observ. Remote Sens.*, vol. 16, pp. 254–266, 2023, doi: 10.1109/JSTARS.2022.3223423.

[12] M. E. Holzman and R. E. Rivas, "Early maize yield forecasting from remotely sensed temperature/vegetation index measurements," *IEEE J. Sel. Topics Appl. Earth Observ. Remote Sens.*, vol. 9, no. 1, pp. 507–519, Jan. 2016, doi: 10.1109/JSTARS.2015.2504262.

[13] L. Li et al., "Developing machine learning models with multi-source environmental data to predict wheat yield in China," *Comput. Electron. Agriculture*, vol. 194, 2022, Art. no. 106790, doi: 10.1016/j.compag.2022.106790.

[14] M. Ullah, F. Islam, and A. Bais, "Quantifying consistency of crop establishment using a lightweight U-net deep learning architecture and image processing techniques," *Comput. Electron. Agriculture*, vol. 217, 2024, Art. no. 108617, doi: 10.1016/j.compag.2024.108617.

[15] G. Cheng, X. Xie, J. Han, L. Guo, and G.-S. Xia, "Remote sensing image scene classification meets deep learning: Challenges, methods, benchmarks, and opportunities," *IEEE J. Sel. Topics Appl. Earth Observ. Remote Sens.*, vol. 13, pp. 3735–3756, 2020, doi: 10.1109/JSTARS.2020.3005403.

[16] B. Hosseiny, M. Mahdianpari, M. Hemati, A. Radman, F. Mohammadimanesh, and J. Chanussot, "Beyond supervised learning in remote sensing: A systematic review of deep learning approaches," *IEEE J. Sel. Topics Appl. Earth Observ. Remote Sens.*, vol. 17, pp. 1035–1052, 2024, doi: 10.1109/JSTARS.2023.3316733.

[17] R. N. Mitchell, "Chang'E-5 reveals the moon's secrets to a longer life," *Innov.*, vol. 2, no. 4, 2021, Art. no. 100177, doi: 10.1016/j.xinn.2021.100177.

[18] J. Guo et al., "Identify urban area from remote sensing image using deep learning method," in *Proc. IEEE Int. Geosci. Remote Sens. Symp.*, 2019, pp. 7407–7410, doi: 10.1109/IGARSS.2019.8898874.

[19] B. Zhang et al., "Progress and challenges in intelligent remote sensing satellite systems," *IEEE J. Sel. Topics Appl. Earth Observ. Remote Sens.*, vol. 15, pp. 1814–1822, 2022, doi: 10.1109/JSTARS.2022.3148139.

[20] M. Qiao et al., "Crop yield prediction from multi-spectral, multi-temporal remotely sensed imagery using recurrent 3D convolutional neural networks," *Int. J. Appl. Earth Observ. Geoinformation*, vol. 102, 2021, Art. no. 102436, doi: 10.1016/j.jag.2021.102436.

[21] X. Wang, J. Huang, Q. Feng, and D. Yin, "Winter wheat yield prediction at county level and uncertainty analysis in main wheat-producing regions of China with deep learning approaches," *Remote Sens.*, vol. 12, no. 11, 2020, Art. no. 1744, doi: 10.3390/rs12111744.

[22] M. Amani et al., "Google Earth engine cloud computing platform for remote sensing Big Data applications: A comprehensive review," *IEEE J. Sel. Topics Appl. Earth Observ. Remote Sens.*, vol. 13, pp. 5326–5350, 2020, doi: 10.1109/JSTARS.2020.3021052.

[23] X. Liu et al., "Large-scale crop mapping from multisource remote sensing images in Google Earth engine," *IEEE J. Sel. Topics Appl. Earth Observ. Remote Sens.*, vol. 13, pp. 414–427, 2020, doi: 10.1109/JSTARS.2019.2963539.

[24] W. Wang, X. Tan, P. Zhang, and X. Wang, "A CBAM based multiscale transformer fusion approach for remote sensing image change detection," *IEEE J. Sel. Topics Appl. Earth Observ. Remote Sens.*, vol. 15, pp. 6817–6825, 2022, doi: 10.1109/JSTARS.2022.3198517.

[25] Z. Zhang and L. Zhu, "A review on unmanned aerial vehicle remote sensing: Platforms, sensors, data processing methods, and applications," *Drones*, vol. 7, no. 6, 2023, Art. no. 398, doi: 10.3390/drones7060398.

[26] A. Gracia-Romero et al., "Comparative performance of ground vs. aerially assessed RGB and multispectral indices for early-growth evaluation of maize performance under phosphorus fertilization," *Front. Plant Sci.*, vol. 8, 2017, Art. no. 2004, doi: 10.3389/fpls.2017.02004.

[27] P. Horstrand, R. Guerra, A. Rodríguez, M. Díaz, S. López, and J. F. López, "A UAV platform based on a hyperspectral sensor for image capturing and on-board processing," *IEEE Access*, vol. 7, pp. 66919–66938, 2019, doi: 10.1109/ACCESS.2019.2913957.

[28] L. Tait, J. Bind, H. Charan-Dixon, I. Hawes, J. Pirker, and D. Schiel, "Unmanned aerial vehicles (UAVs) for monitoring macroalgal biodiversity: Comparison of RGB and multispectral imaging sensors for biodiversity assessments," *Remote Sens.*, vol. 11, no. 19, 2019, Art. no. 2332, doi: 10.3390/rs11192332.

[29] N. Ali, Z. Halim, and S. F. Hussain, "An artificial intelligence-based framework for data-driven categorization of computer scientists: A case study of world's top 10 computing departments," *Scientometrics*, vol. 128, no. 3, pp. 1513–1545, 2023, doi: 10.1007/s11192-022-04627-9.

[30] A. Verger, N. Vigneau, C. Chéron, J.-M. Gilliot, A. Comar, and F. Baret, "Green area index from an unmanned aerial system over wheat and rapeseed crops," *Remote Sens. Environ.*, vol. 152, pp. 654–664, 2014, doi: 10.1016/j.rse.2014.06.006.

[31] H. Ashfaq et al., "Mitigating crop losses: AI-enabled disease detection in tomato plants," in *Proc. Int. Conf. Frontier Inf. Technol.*, 2023, pp. 190–195, doi: 10.1109/FIT60620.2023.00043.

[32] F. Pei, Y. Zhou, and Y. Xia, "Application of normalized difference vegetation index (NDVI) for the detection of extreme precipitation change," *Forests*, vol. 12, no. 5, 2021, Art. no. 594, doi: 10.3390/f12050594.

[33] Z. Jiang, A. R. Huete, K. Didan, and T. Miura, "Development of a two-band enhanced vegetation index without a blue band," *Remote Sens. Environ.*, vol. 112, no. 10, pp. 3833–3845, 2008, doi: 10.1016/j.rse.2008.06.006.

[34] H. Zheng et al., "A comparative assessment of different modeling algorithms for estimating leaf nitrogen content in winter wheat using multispectral images from an unmanned aerial vehicle," *Remote Sens.*, vol. 10, no. 12, 2018, Art. no. 2026, doi: 10.3390/rs10122026.

[35] X. Zhou et al., "Predicting grain yield in rice using multi-temporal vegetation indices from UAV-based multispectral and digital imagery," *ISPRS J. Photogrammetry Remote Sens.*, vol. 130, pp. 246–255, 2017, doi: 10.1016/j.isprsjprs.2017.05.003.

[36] W. Zhu, S. Li, X. Zhang, Y. Li, and Z. Sun, "Estimation of winter wheat yield using optimal vegetation indices from unmanned aerial vehicle remote sensing," *Trans. Chin. Soc. Agricultural Eng.*, vol. 34, pp. 78–86, 2018. [Online]. Available: https://www.cabidigitallibrary.org/doi/full/10.5555/20183255026

[37] Z. Fu et al., "Wheat growth monitoring and yield estimation based on multi-rotor unmanned aerial vehicle," *Remote Sens.*, vol. 12, no. 3, 2020, Art. no. 508, doi: 10.3390/rs12030508.

[38] S. Shafiee, L. M. Lied, I. Burud, J. A. Dieseth, M. Alsheikh, and M. Lillemo, "Sequential forward selection and support vector regression in comparison to LASSO regression for spring wheat yield prediction based on UAV imagery," *Comput. Electron. Agriculture*, vol. 183, 2021, Art. no. 106036, doi: 10.1016/j.compag.2021.106036.

[39] L. Wan et al., "Grain yield prediction of rice using multi-temporal UAV-based RGB and multispectral images and model transfer—A case study of small farmlands in the south of China," *Agricultural Forest Meteorol.*, vol. 291, 2020, Art. no. 108096, doi: 10.1016/j.agrformet.2020.108096.

[40] C. van Diepen, J. Wolf, H. van Keulen, and C. Rappoldt, "WOFOST: A simulation model of crop production," *Soil Use Manage.*, vol. 5, no. 1, pp. 16–24, 1989, doi: 10.1111/j.1475-2743.1989.tb00755.x.

[41] J. Jones et al., "The DSSAT cropping system model," *Eur. J. Agronomy*, vol. 18, no. 3, pp. 235–265, 2003, doi: 10.1016/S1161-0301(02)00107-7.

[42] R. McCown, G. Hammer, J. Hargreaves, D. Holzworth, and D. Freebairn, "APSIM: A novel software system for model development, model testing and simulation in agricultural systems research," *Agricultural Syst.*, vol. 50, no. 3, pp. 255–271, 1996, doi: 10.1016/0308-521X(94)00055-V.

[43] V. Manivasagam and O. Rozenstein, "Practices for upscaling crop simulation models from field scale to large regions," *Comput. Electron. Agriculture*, vol. 175, Art. no. 105554, 2020, doi: 10.1016/j.compag.2020.105554.

[44] F. Islam, M. Ullah, and A. Bais, "Quancro: A novel framework for quantification of corn crops' consistency under natural field conditions," *Neural Comput. Appl.*, vol. 35, no. 35, pp. 24877–24896, 2023, doi: 10.1007/s00521-023-08961-8.

[45] N. Ali, S. Ansari, Z. Halim, R. H. Ali, M. F. Khan, and M. Khan, "Breast cancer classification and proof of key artificial neural network terminologies," in *Proc. 13th Int. Conf. Math., Actuarial Sci., Computer Sci. Statist.*, 2019, pp. 1–6, doi: 10.1109/MACS48846.2019.9024769.

[46] T. M. Mitchell, "Does machine learning really work?," *AI Mag.*, vol. 18, no. 3, p. 11, 1997.

[47] M. J. Roberts, N. O. Braun, T. R. Sinclair, D. B. Lobell, and W. Schlenker, "Comparing and combining process-based crop models and statistical models with some implications for climate change," *Environ. Res. Lett.*, vol. 12, no. 9, Sep. 2017, Art. no. 095010, doi: 10.1088/1748-9326/aa7f33.

[48] A. Abdullah, N. Ali, R. H. Ali, Z. Ul Abideen, A. Z. Ijaz, and A. Bais, "American sign language character recognition using convolutional neural networks," in *Proc. IEEE Can. Conf. Elect. Comput. Eng.*, 2023, pp. 165–169, doi: 10.1109/CCECE58730.2023.10288799.

[49] J. Behmann, A.-K. Mahlein, T. Rumpf, C. Römer, and L. Plümer, "A review of advanced machine learning methods for the detection of biotic stress in precision crop protection," *Precis. Agriculture*, vol. 16, pp. 239–260, 2015, doi: 10.1007/s11119-014-9372-7.

[50] W. Zhou, Y. Liu, S. T. Ata-Ul-Karim, Q. Ge, X. Li, and J. Xiao, "Integrating climate and satellite remote sensing data for predicting county-level wheat yield in China using machine learning methods," *Int. J. Appl. Earth Observ. Geoinformation*, vol. 111, 2022, Art. no. 102861, doi: 10.1016/j.jag.2022.102861.

[51] N. Ali, A. Z. Ijaz, R. H. Ali, Z. Ul Abideen, and A. Bais, "Scene parsing using fully convolutional network for semantic segmentation," in *Proc. IEEE Can. Conf. Elect. Comput. Eng.*, 2023, pp. 180–185, doi: 10.1109/CCECE58730.2023.10288934.

[52] T. van Klompenburg, A. Kassahun, and C. Catal, "Crop yield prediction using machine learning: A systematic literature review," *Comput. Electron. Agriculture*, vol. 177, 2020, Art. no. 105709, doi: 10.1016/j.compag.2020.105709.

[53] J. H. Jeong et al., "Random forests for global and regional crop yield predictions," *PLoS One*, vol. 11, no. 6, 2016, Art. no. e0156571, doi: 10.1371/journal.pone.0156571.
[54] G. Leng and J. W. Hall, "Predicting spatial and temporal variability in crop yields: An inter-comparison of machine learning, regression and process-based models," *Environ. Res. Lett.*, vol. 15, no. 4, Apr. 2020, Art. no. 044027, doi: 10.1088/1748-9326/ab7b24.
[55] J. Cao et al., "Wheat yield predictions at a county and field scale with deep learning, machine learning, and Google Earth engine," *Eur. J. Agronomy*, vol. 123, 2021, Art. no. 126204, doi: 10.1016/j.eja.2020.126204.
[56] P. Filippi et al., "An approach to forecast grain crop yield using multi-layered, multi-farm data sets and machine learning," *Precis. Agriculture*, vol. 20, pp. 1015–1029, 2019, doi: 10.1007/s11119-018-09628-4.
[57] V. Sagan et al., "Field-scale crop yield prediction using multi-temporal WorldView-3 and PlanetScope satellite data and deep learning," *ISPRS J. Photogrammetry Remote Sens.*, vol. 174, pp. 265–281, 2021, doi: 10.1016/j.isprsjprs.2021.02.008.
[58] A. Chlingaryan, S. Sukkarieh, and B. Whelan, "Machine learning approaches for crop yield prediction and nitrogen status estimation in precision agriculture: A review," *Comput. Electron. Agriculture*, vol. 151, pp. 61–69, 2018, doi: 10.1016/j.compag.2018.05.012.
[59] S. S. Panda, D. P. Ames, and S. Panigrahi, "Application of vegetation indices for agricultural crop yield prediction using neural network techniques," *Remote Sens.*, vol. 2, no. 3, pp. 673–696, 2010, doi: 10.3390/rs2030673.
[60] A. P. Professional, "Discover intelligent photogrammetry with metashape," 2010. [Online]. Available: https://www.agisoft.com/
[61] K. Kingsland, "Comparative analysis of digital photogrammetry software for cultural heritage," *Digit. Appl. Archaeol. Cultural Heritage*, vol. 18, 2020, Art. no. e00157, doi: 10.1016/j.daach.2020.e00157.
[62] QGIS Development Team, "QGIS geographic information system, open source geospatial foundation," 2009. [Online]. Available: http://qgis.osgeo.org
[63] N. Moyroud and F. Portet, *Introduction to QGIS*. Hoboken, NJ, USA: Wiley, 2018, ch. 1, pp. 1–17, doi: 10.1002/9781119457091.ch1.
[64] M. Reynolds, A. Pask, and D. Mullan, *Physiological Breeding I: Interdisciplinary Approaches to Improve Crop Adaptation*. El Batán, Mexico: CIMMYT, 2012.
[65] N. Ali, A. Mohammed, A. Bais, J. S. Sangha, Y. Ruan, and R. D. Cuthbert, "LodgeNet: An automated framework for precise detection and classification of wheat lodging severity levels in precision farming," *Front. Plant Sci.*, vol. 14, 2023, Art. no. 1255961, doi: 10.3389/fpls.2023.1255961.
[66] CVAT.ai Corporation, "Computer vision annotation tool (CVAT)," Nov. 2023. [Online]. Available: https://github.com/opencv/cvat
[67] L. Rokach and O. Maimon, *Decision trees*. Boston, MA, USA: Springer, 2005, pp. 165–192, doi: 10.1007/0-387-25465-X_9.
[68] M. Belgiu and L. Drăguţ, "Random forest in remote sensing: A review of applications and future directions," *ISPRS J. Photogrammetry Remote Sens.*, vol. 114, pp. 24–31, 2016, doi: 10.1016/j.isprsjprs.2016.01.011.
[69] C. Bentéjac, A. Csörg, and G. Martínez-Muñoz, "A comparative analysis of gradient boosting algorithms," *Artif. Intell. Rev.*, vol. 54, pp. 1937–1967, 2021, doi: 10.1007/s10462-020-09896-5.
[70] T. Chen et al., "XGBoost: Extreme gradient boosting," *R Package Version 0.4-2*, vol. 1, no. 4, pp. 1–4, 2015.
[71] T. Thomas, A. P. Vijayaraghavan, and S. Emmanuel, *Applications of Decision Trees*. Singapore: Springer, 2020, pp. 157–184, doi: 10.1007/978-981-15-1706-8_9.
[72] J. Brophy and D. Lowd, "Machine unlearning for random forests," in *Proc. 38th Int. Conf. Mach. Learn.*, 2021, pp. 1092–1104. [Online]. Available: https://proceedings.mlr.press/v139/brophy21a.html
[73] R. Sibindi, R. W. Mwangi, and A. G. Waititu, "A boosting ensemble learning based hybrid light gradient boosting machine and extreme gradient boosting model for predicting house prices," *Eng. Rep.*, vol. 5, no. 4, 2023, Art. no. e12599. [Online]. Available: https://onlinelibrary.wiley.com/doi/abs/10.1002/eng2.12599
[74] Y. Wu, H. Huang, W. Xu, and J. Huang, "Field scale winter wheat yield estimation with Sentinel-2 data and a process based model," in *Proc. IEEE Int. Geosci. Remote Sens. Symp.*, 2022, pp. 6065–6068, doi: 10.1109/IGARSS46834.2022.9883533.
[75] J. Han et al., "Prediction of winter wheat yield based on multi-source data and machine learning in China," *Remote Sens.*, vol. 12, no. 2, 2020, Art. no. 236, doi: 10.3390/rs12020236.
[76] X. Wang et al., "Modelling rice yield with temperature optima of rice productivity derived from satellite NIRv in tropical monsoon area," *Agricultural Forest Meteorol.*, vol. 294, 2020, Art. no. 108135, doi: 10.1016/j.agrformet.2020.108135.
[77] J. Cao et al., "Integrating multi-source data for rice yield prediction across China using machine learning and deep learning approaches," *Agricultural Forest Meteorol.*, vol. 297, 2021, Art. no. 108275, doi: 10.1016/j.agrformet.2020.108275.
[78] P. Feng et al., "Dynamic wheat yield forecasts are improved by a hybrid approach using a biophysical model and machine learning technique," *Agricultural Forest Meteorol.*, vol. 285/286, 2020, Art. no. 107922, doi: 10.1016/j.agrformet.2020.107922.
[79] P. S. M. Gopal and R. Bhargavi, "Performance evaluation of best feature subsets for crop yield prediction using machine learning algorithms," *Appl. Artif. Intell.*, vol. 33, no. 7, pp. 621–642, 2019, doi: 10.1080/08839514.2019.1592343.
[80] T. Sakamoto, "Incorporating environmental variables into a MODIS-based crop yield estimation method for United States corn and soybeans through the use of a random forest regression algorithm," *ISPRS J. Photogrammetry Remote Sens.*, vol. 160, pp. 208–228, 2020, doi: 10.1016/j.isprsjprs.2019.12.012.
[81] S. Khanal, J. Fulton, A. Klopfenstein, N. Douridas, and S. Shearer, "Integration of high resolution remotely sensed data and machine learning techniques for spatial prediction of soil properties and corn yield," *Comput. Electron. Agriculture*, vol. 153, pp. 213–225, 2018, doi: 10.1016/j.compag.2018.07.016.
[82] G. Badagliacca et al., "Multispectral vegetation indices and machine learning approaches for durum wheat (Triticum durum desf.) yield prediction across different varieties," *AgriEngineering*, vol. 5, no. 4, pp. 2032–2048, 2023, doi: 10.3390/agriengineering5040125.
[83] J. Cao et al., "Identifying the contributions of multi-source data for winter wheat yield prediction in China," *Remote Sens.*, vol. 12, no. 5, 2020, Art. no. 750, doi: 10.3390/rs12050750.
[84] J. Huang, H. Wang, Q. Dai, and D. Han, "Analysis of NDVI data for crop identification and yield estimation," *IEEE J. Sel. Topics Appl. Earth Observ. Remote Sens.*, vol. 7, no. 11, pp. 4374–4384, Nov. 2014, doi: 10.1109/JSTARS.2014.2334332.
[85] L. Prey, Y. Hu, and U. Schmidhalter, "High-throughput field phenotyping traits of grain yield formation and nitrogen use efficiency: Optimizing the selection of vegetation indices and growth stages," *Front. Plant Sci.*, vol. 10, 2020, Art. no. 1672, doi: 10.3389/fpls.2019.01672.

Nisar Ali (Student Member, IEEE) received the B.Sc. (Hons.) degree in computer science from the University of Bradford, Bradford, U.K., in 2018 and the master's degree (with distinction) in computer science from the Ghulam Ishaq Khan Institute of Engineering Sciences and Technology, Topi, Pakistan, in 2021. He is currently working toward the Ph.D. degree in faculty of engineering and applied science from University of Regina, Regina, SK, Canada.

His Ph.D. research focuses on precision agriculture.

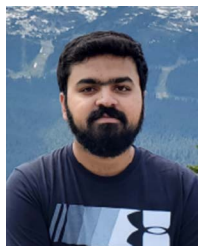

Ahmed Mohammed (Student Member, IEEE) received the bachelor's degree in electrical engineering from COMSATS University, Lahore, Pakistan, in 2020. He is currently working toward the MASc degree in electronic systems engineering with the University of Regina, Regina, SK, Canada.

He is currently a Graduate Research Student with the University of Regina. His research focuses on the application of computer vision in agriculture.

Abdul Bais (Senior Member, IEEE) received the B.Sc. and M.Sc. degrees in electrical engineering from the University of Engineering and Technology, Peshawar, Pakistan, in 2000 and 2003, respectively. He completed his Ph.D. in electrical engineering and information technology at Vienna University of Technology, Vienna, Austria in 2007.

From 2010 to 2013, he was a postdoctoral fellow at the Faculty of Engineering and Applied Science, University of Regina, Saskatchewan, Canada.

Dr. Bais is a certified instructor with the NVIDIA Deep Learning Institute and a Licensed Professional Engineer in the State of Saskatchewan, Canada.

Samia Berraies received the Ph.D. degree in plant pathology from the University of Tunis, Tunis, Tunisia, in 2014.

She is currently a Cereal Pathologist with Agriculture and Agri-Food Canada's Swift Current Research and Development Centre, Swift Current, SK, Canada. She collaborates closely with wheat breeders to develop new wheat varieties with enhanced genetic resilience. Her current research focuses on unraveling the genetic factors associated with resistance to wheat diseases, particularly Fusarium head blight and ergot.

Yuefeng Ruan received the Ph.D. degree in agriculture (plant nutrition) from the Technical University of Munich, Munich, Germany, in 2007. He is currently a Senior Research Scientist and Durum Wheat Breeder with Swift Current Research and Development Centre, AAFC, Swift Current, SK, Canada. He has registered 12 durum wheat cultivars, including the first Intermediate Fusarium Head Blight resistance cultivar and the first wheat midge and wheat stem sawfly insect resistance cultivar in Canada. He has authored or coauthored hundreds of miscellaneous publications in wheat breeding and research. His research and breeding program develops new high-quality and high-yielding durum wheat cultivars with wide adaptability and improved profitability.

Dr. Ruan provides the leadership in durum wheat research and development as an active member of numerous government and nongovernment committees in Canada and worldwide.

Richard D. Cuthbert received the Ph.D. degree specializing in molecular biology and plant pathology from the University of Manitoba, Winnipeg, MB, Canada, in 2011.

He is currently a wheat breeder with Agriculture and Agri-Food Canada, Swift Current Research and Development Centre, Swift Current, SK, Canada. His research interest includes developing new wheat varieties with improved genetics for biotic and abiotic stresses, as well as implementing new technologies in the wheat breeding process.

Jatinder S. Sangha received the Ph.D. degree in plant science from the University of the Philippines, Los Banos, Philippines, in 2006.

He is currently a Research Scientist with Agriculture and Agri-Food Canada's Research and Development Centre, Swift Current, SK, Canada. His expertise involves crop physiology (abiotic stresses), plant phenomics, grain quality, and host plant resistance. His ongoing research aims to develop phenotyping procedures for the application of physiological breeding in wheat to improve yield reliability and grain quality under diverse field environments. His research also investigates physiological and genetic mechanisms of heat and drought stress tolerance, nitrogen use efficiency, and dry down in wheat.